USGS
science for a changing world

Prepared for the National Aeronautics and Space Administration

Geologic Map of the Guinevere Planitia Quadrangle (V–30), Venus

By David A. Crown, Ellen R. Stofan, and Leslie F. Bleamaster III

Pamphlet to accompany
Scientific Investigations Map 3539

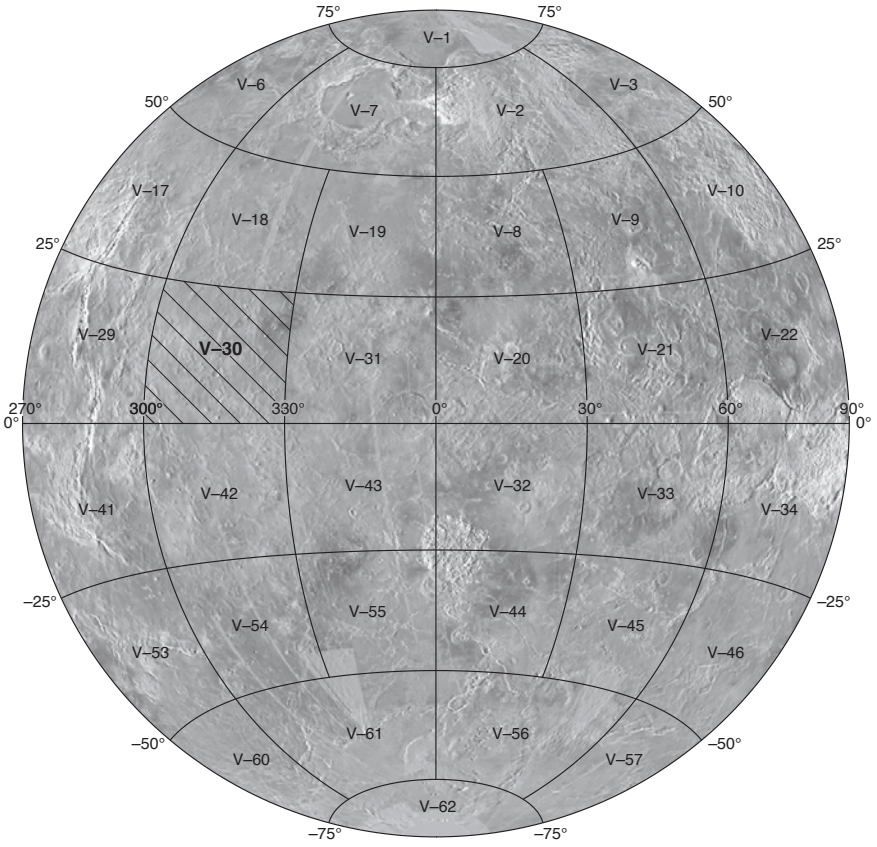

2025

U.S. Department of the Interior
U.S. Geological Survey

U.S. Geological Survey, Reston, Virginia: 2025

Suggested citation:
Crown, D.A., Stofan, E.R., Bleamaster, L.F., III, 2025, Geologic map of the Guinevere Planitia quadrangle (V-30), Venus: U.S. Geological Survey Scientific Investigations Map 3539, 1 sheet, scale 1:5,000,000, pamphlet 15 p., https://doi.org/10.3133/sim3539.

ISSN 2329-1311 (print)
ISSN 2329-132X (online)

Cover. Globe location map showing location of map area (hachured area). Photomosaic from Magellan synthetic aperture radar. An outline of 1:5,000,000-scale quadrangles is provided for reference.

Contents

Figures

Tables

Geologic Map of the Guinevere Planitia Quadrangle (V–30), Venus

By David A. Crown, Ellen R. Stofan, and Leslie F. Bleamaster III

Introduction

Guinevere Planitia is an expansive lowland region in the northern low to mid-latitudes of Venus, between Sedna Planitia to the north, Navka Planitia to the south, Beta Regio to the southwest, and Eistla Regio to the east. The Guinevere Planitia quadrangle (V–30; spanning lat 0–25° N. and long 300–330° E.) includes parts of Guinevere Planitia and Undine Planitia, which are dominated by low-lying plains interpreted to be of volcanic origin. The quadrangle also contains a suite of other volcanic landforms, including volcanoes, coronae, lava channels, and many small volcanic edifices (Head and others, 1992; Tanaka and others, 1997). Previous analyses using Pioneer Venus, Goldstone, and Arecibo radar data described radar bright, dark, and mottled plains and the arcuate fracture zones and lineament belt segments that define the Beta-Eistla deformation zone (Campbell and others, 1989; Arvidson and others, 1990; Stofan and others, 1990; Senske, 1990; Senske and others, 1991). Geologic investigations using Magellan synthetic aperture radar (SAR) data, including this mapping study, have revealed the nature and history of the geologic events that have shaped this region of the Venusian surface (Crown and others, 1993, 1994, 2008a, b, 2011; Brian and others, 2004; Crown and Stofan, 2006).

Given the abundance and diversity of volcanic features in the Guinevere Planitia quadrangle, our primary scientific objective was to examine the styles and history of Venusian volcanism as recorded in its predominantly volcanic landscape. Volcanic landforms such as shield volcanoes, widespread plains, lava flow fields, lava channels, and a variety of small, domes, cones, and shields, both isolated and found in clusters, were identified in the quadrangle. In addition, coronae and other circular features in the quadrangle are apparent sources for adjacent volcanic flow units. Specific research foci of our geologic mapping analyses included the volcanic and tectonic evolution of Venusian plains, the styles and temporal sequences of volcanism at the major eruptive centers (shield volcanoes and coronae), and the geologic context for steep-sided dome formation in the plains and on shield volcanoes. Research related to this geologic mapping also included morphologic and remote sensing studies of steep-sided domes on Venus and analyses of terrestrial silicic domes as potential analogs for these Venusian features (see Anderson and others, 1998; Stofan and others, 2000; Plaut and others, 2004). Additional investigations included morphologic and radar backscatter characteristics of lava flows associated with volcanoes in Guinevere Planitia (refer to Byrnes and Crown, 2002).

In our mapping of the Guinevere Planitia quadrangle at a 1:5,000,000 scale, we divided the region into 15 geologic material units and 4 groups. These groups consist of upland terrain, plains materials, flow materials (associated with named and unnamed eruptive centers), and other materials (a small volcanic edifice unit and an impact crater material unit). The Guinevere Planitia quadrangle contains four major volcanoes: Atanua Mons, Tuli Mons, and Var Mons, the three of which form an elongate topographic rise termed Laufey Regio (Brian and others, 2004), and part of a fourth volcano named Rhpisunt Mons. Other features on or near Laufey Regio include Uilata Fluctus, Koti Fluctus, and Mehseti Patera. Several coronae are present: Hulda Corona is adjacent to Atanua Mons, Madderakka Corona lies between Var Mons and Tuli Mons, and part of Pölöznitsa Corona is visible in the southwest corner of the quadrangle. Nine impact craters are found within the Guinevere Planitia quadrangle, such as Seymour, a crater in the northeast area of the quadrangle that is surrounded by extensive ejecta outflow deposits. Deformed terrains are found in Kalm Dorsa (northwest of Tuli Mons) and in Nang-byon Chasma (on Var Mons in the south part of the quadrangle). Table 1 lists the sizes and locations of named features in the Guinevere Planitia quadrangle; their morphologic and morphometric descriptions are provided in the "Geology of the Guinevere Planitia Quadrangle" section.

The Magellan Mission

This section has been reproduced with minor edits from text prepared for the 1:5,000,000-scale quadrangle series of Venus geologic maps. Similar versions appear in other map publications, including geologic maps of the V–35 and V–53 quadrangles (Bleamaster and Hansen, 2005 and Stofan and Brian, 2012, respectively).

The Magellan spacecraft (refer to Saunders and others, 1992) orbited Venus from August 10, 1990, until it plunged into the Venusian atmosphere on October 12, 1994. Magellan had two objectives: (1) to improve knowledge of the geologic processes, surface properties, and geologic history of Venus by analyzing its surface radar characteristics, topography, and morphology; and (2) to improve knowledge of the geophysics of Venus by analyzing Venusian gravity.

Table 1. Named features in the Guinevere Planitia quadrangle of Venus.

[km, kilometer; ° N., degrees north; ° E., degrees east. From Gazetteer of Planetary Nomenclature (https://planetarynames.wr.usgs.gov)]

Name	Diameter (km)	Center Latitude (° N.)	Center Longitude (° E.)	Name Origin
Guinevere Planitia	7,520	21.9	325.0	British, wife of Arthur
Undine Planitia	2,800	13.0	303.0	Lithuanian water nymph, mermaid
Laufey Regio	2,100	7.0	315.0	Norse giantess
Caroline crater	18	6.9	306.3	First name from French
Gudrun crater	13	10.6	326.4	First name from Norse
Kala crater	17	1.5	314.4	Koryak (Kamchatka) first name
Ketzia crater	15	3.9	300.5	Hebrew first name
Neda crater	8	16.7	313.5	Macedonian first name
Potter crater	47	7.2	309.1	Beatrix; English children's author
Seymour crater	63	18.2	326.5	Jane; English queen
Shih Mai-Yu crater	22	18.4	318.9	Chinese physician
Vard crater	6	17.5	314.5	Armenian first name
Hulda Corona	230	12.0	308.3	German goddess of fruitfulness and marriage
Madderakka Corona	220	9.0	315.5	Lapp goddess of birth
Pölöznitsa Corona	675	0.5	302.0	Finno-Ugric grain goddess
Atanua Mons	1,000	9.5	308.9	Dawn goddess from Marquesas Islands
Rhpisunt Mons	250	2.5	301.5	Haida (Northwest Coast) Bear Mother deity
Tuli Mons	750	13.3	314.6	Samoan goddess of creation
Var Mons	1,000	1.2	316.2	Scandinavian love goddess
Koti Fluctus	400	12.5	318.0	Creek (SE USA) water-frog, helpful spirit
Uilata Fluctus	700	17.0	314.0	Cherokee stone-clad female monster
Mehseti Patera	60	16.0	311.0	Ganjevi; Azeri/Persian poetess
Kalm Dorsa	300	18.0	309.0	Mansi (Ob River Ugra) winged messenger from gods to humans
Nang-byon Chasma	450	4.0	316.5	Thaichang/White Thai (Vietnam) Moon goddess
Tingoi Vallis	250	6.0	318.6	Mande (Sierra Leone) river spirit

The Magellan spacecraft carried a 12.6-centimeter- (cm) wavelength radar system to map the surface of Venus. The transmitter and receiver systems were used to collect three datasets: SAR images of the surface, passive microwave thermal emission observations, and measurements of the backscattered power at small angles of incidence, which were processed to yield altimetric data. Radar imaging, altimetric mapping, and radiometric mapping of the Venusian surface were done in mission cycles 1, 2, and 3, from September 1990 until September 1992. Ninety-eight percent of the surface was mapped with a radar resolution of ~120 meters (m). The SAR observations were projected to a 75-m nominal horizontal resolution; these full-resolution data compose the image base used in our geologic mapping. The primary polarization mode was horizontal transmit, horizontal receive (HH), but additional data for selected areas were collected for the vertical polarization sense. Incidence angles varied from about 20° to 45°.

High-resolution Doppler tracking of the spacecraft took place from September 1992 through October 1994 (mission cycles 4, 5, and 6). High-resolution gravity observations from about 950 orbits were obtained between September 1992 and May 1993 while Magellan was in an elliptical orbit, with a periapsis near 175 kilometers (km) and apoapsis near 8,000 km. Observations from an additional 1,500 orbits were obtained after orbit circularization in mid-1993. These data exist as a 75° by 75° harmonic field.

Magellan Radar Data

Radar backscatter power is determined by the morphology of the surface at a broad range of scales and by the intrinsic reflectivity, or dielectric constant, of the material. Topography at scales of several meters or larger can produce quasi-specular echoes, with the strength of the return greatest where the local surface is perpendicular to the incident beam. This kind of scattering is most conspicuous at small angles of incidence because natural surfaces generally have few large faces tilted at high angles. The exception is in steeply sloping areas, such as ridges or rift zones, where favorably tilted terrain can produce very bright signatures in radar images. For most other areas, variations in the SAR return are the result of diffuse echoes produced by roughness at scales comparable to the radar wavelength. In either

instance, the echo strength is also modulated by the reflectivity of the surface material. Another factor that can have a significant effect is the density of surficial materials—those located from the surface to the depth of a few wavelengths. Low-density surficial layers, such as crater ejecta or volcanic ash, can absorb the incident energy and produce a weaker observed echo. On Venus, a rapid increase in reflectivity exists at a certain critical elevation, above which high-dielectric minerals or coatings are thermodynamically stable. This effect leads to very bright SAR echoes from virtually all areas above that critical elevation.

The measurements of passive thermal emissions from Venus, although of much lower spatial resolution than the SAR data, are more sensitive to changes in surficial dielectric constant than to roughness. As such, they can be used to augment studies of the surface and to discriminate between roughness and reflectivity effects. Observations of the near-nadir backscatter power, collected using a separate, smaller antenna on the spacecraft, were modeled using Hagfors' expression (Hagfors, 1964) for echoes from gently undulating surfaces to produce estimates of planetary radius, Fresnel reflectivity, and root mean square (rms) slope. The topography data produced by this technique have horizontal footprint sizes of about 10 km near periapsis and a vertical resolution of ~100 m. The Fresnel reflectivity data provide another comparison to the emissivity maps, and the rms slope parameter acts as an indicator of surficial tilts, which contribute to the quasi-specular scattering component.

Methods and Data

To construct the geologic map of the Guinevere Planitia quadrangle, we used standard planetary geologic mapping techniques for identifying, describing, and portraying geologic units, geologic features, and surficial deposits (Wilhelms, 1972, 1990; Hansen, 1991). Magellan SAR data (12.6-cm radar system; 75 m per pixel) served as the map base. More than 90 percent of the quadrangle is covered by left-looking and right-looking SAR images; data gaps are displayed as north-south white strips. The left-looking mosaic was used as the primary mapping base. We used SAR images and altimetry as well as roughness (rms slope), reflectivity, and emissivity datasets (figs. 1, 2) to describe the regional geology (Pettengill and others, 1992; Campbell, 1995). The scale and nature of these additional datasets are not conducive to geologic unit delineation in this study, but they are useful for regional comparison and thus have been included as figures.

Magellan Digital Full-Resolution Radar Maps (F-MAPs; image mosaics created from Magellan Full-Resolution Basic Image Data Records or F-BIDRs) and synthetic parallax stereo images (with 10 times vertical exaggeration), produced by the U.S. Geological Survey, were used as key mapping products for unit characterization and delineation, and for the determination of stratigraphic relationships, cross-cutting relationships, and volcanic flow emplacement directions. The geologic contacts on the map generally represent well-defined boundaries between adjacent units as indicated by radar backscatter differences, changes in the pattern or density of geologic features, or both. We used approximate contacts in areas where the contact positions were difficult to determine because of a lack of distinct backscatter differences at unit boundaries. We have included documentation of local superposition relationships between younger (Y) and older (O) units in key locations, as well as at internal contacts (where different exposures of the same unit meet). This map was initially compiled in a nonspatial vector drafting software and was subsequently converted into a geographic information system (GIS) format. Some contact positions were refined in the GIS to accurately correspond to the map base. Some contacts were also reshaped to produce smooth lines appropriate to the map scale.

Left-looking and right-looking SAR images are available for most of the quadrangle and allow more than 90 percent of the surface area to be characterized in both datasets; however, a small part of the quadrangle is covered by only right-looking SAR images (shown as north-south strips east of lat 320° E.). Where possible, these data were used to extend the mapping of geologic units and features into data gaps in the primary base map of left-looking SAR images. The presence of true data gaps (that is, areas with no left- or right-looking images) prevented us from defining geologic units and features across the full extent of the quadrangle. Nonetheless, we extrapolated our mapping across the small but numerous data gaps in the central part of the quadrangle, and in the narrow, elongate data gaps to the southeast. The areas of extrapolation are clearly recognizable as bands of lighter shading on the geologic map sheet, and the reader can readily determine where we extrapolated across data gaps. Larger data gaps and areas for which we felt extrapolation was not warranted are shown in white. The "inferred contact" symbol is used for all contacts extrapolated across data gaps.

Many prior studies have used radar datasets to characterize the nature of Venus' volcanic surfaces, describe the morphologies of its volcanic landforms, and infer the nature of its volcanic processes (Head and Wilson, 1986; Campbell and Campbell, 1992; Campbell and others, 1993; Campbell and Rogers, 1994; Byrnes and Crown, 2002). The ability to make geologic maps primarily from radar data depends on the spatial resolution available, and unit discrimination can be hindered if variability in radar backscatter is low or does not directly relate to material units (Ford and others, 1993). A geologic contact will only be visible in radar data if the adjacent units have different backscatter characteristics; this may not occur everywhere, particularly in volcanic terrains. Radar backscatter can also vary within a single geologic unit (for example, a lava flow) as a result of cooling, changes in the flow emplacement regime, or both, that can cause differences in texture or morphology that would have different backscatter characteristics. Thus, it is important to consider geologic context when defining units so as not to erroneously map them solely on the basis of radar backscatter. In addition, adjacent units of different ages can have similar radar backscatter characteristics, and so may mistakenly be combined into a single geologic unit. Structural features are often more apparent if they are oriented perpendicular to the radar look-direction (Stofan and others, 1989). In Magellan data, north-south trending lineaments may be more evident and east-west trending features underrepresented simply because of their orientations.

Elevations within the Guinevere Planitia quadrangle typically range between −1 and 1 km (mean elevation of 800 m) relative to the mean planetary radius of 6,051 km (Pettengill and others, 1991). The highest elevations are associated with the summits of the major volcanoes: Atanua, Rhpisunt, and Var Montes (figs. 1b,

2a). Elevations vary across the quadrangle, and low-lying terrains of Guinevere Planitia are generally located in the north, northeast, and east. The topographic characteristics of the central, south, and southwest parts of the quadrangle are variable at the ~200-km scale because of the presence and overlapping nature of major and minor volcanic centers. Coronae appear as both local topographic highs (such as Hulda Corona) and lows (such as Madderakka Corona).

The rms slope, an indicator of meter-scale surface roughness, ranges between 0.33–11.27 in the quadrangle (fig. 2b). The lowest values of rms slope at large scales correspond to the low-lying terrain of Guinevere Planitia itself, which appears smooth in SAR images. The rms slope shows a high degree of local variability in the rest of the map region. Higher values are associated with deformed terrains, including upland terrain and corona margins, along with some volcanic centers. The rms slope generally decreases from the summit areas toward the flanks of the major volcanoes.

Reflectivity, which can be useful for constraining surface composition, is generally low across the Guinevere Planitia quadrangle with an overall range of 0.01–0.24 (fig. 2c). Local zones of higher reflectivity are found in several areas of the quadrangle, including parts of Koti Fluctus and Tuli Mons, the flow material northwest of Hulda Corona (which also includes a dark halo), and an exposure of plains along the north boundary of the map region. On Venus as a whole, high reflectivity at high elevations has been attributed to chemical weathering; the presence of secondary mineral assemblages stable at high elevations affects the dielectric constant (Klose and others, 1992).

Emissivity in the Guinevere Planitia quadrangle ranges between 0.62–0.90 (fig. 2D). Klose and others (1992) indicated that emissivity measurements at low elevations on Venus are typically near the planetary average of ~0.875. On Venus, emissivity and reflectivity are inversely correlated; that is, high reflectivity corresponds to low emissivity, as well as to high dielectric constant (Klose and others, 1992). In the Guinevere Planitia quadrangle, higher values of emissivity correspond to the presence of coronae and corona-like structures, crater outflows, upland terrain, and some flow materials. Lower values of emissivity are associated with volcanic flows and plains materials, including the flanks of the major volcanoes.

Geology of the Guinevere Planitia Quadrangle

We divided the geologic units of the Guinevere Planitia quadrangle into the following groups, with percent surface area shown in parentheses: upland terrain (2.4 percent), plains materials (59 percent), flow materials (37.2 percent), and other materials (including crater materials and the small volcanic edifice unit; 1.4 percent). The quadrangle is largely dominated by plains and flow materials, some of which form the flanks of the observed major volcanoes, and which together surround small and typically isolated exposures of upland terrain. In addition, nine impact craters are scattered across the region. The types, numbers, and patterns of the mapped tectonic features and small volcanic landforms provide valuable details for interpreting the evolution of the landscape.

In the following sections, we describe each of the mapped geologic units, geologic features (linear and point features), and surficial materials (bright and dark halos). Integrated into these descriptions are comparisons to other geologic mapping studies of Venus, particularly the adjacent V–31 quadrangle, and to studies of specific units and features with widespread occurrence on Venus.

Upland Terrain

Scattered throughout the map region are remnants of intensely deformed materials that are generally radar bright. Those showing two or more tectonic fabrics were mapped as tessera (unit t; plural tesserae); those showing one dominant orientation of lineaments were mapped as lineated upland material (unit ul) (figs. 3, 4). Lineated upland material is also found within Hulda Corona.

In the Sif Mons quadrangle (V–31) directly to the east, one can observe similar deformed materials, which Copp and Guest (2007) mapped as tessera material (their unit "t") and deformed plains material (their unit "pd"), respectively. Other 1:5,000,000-scale quadrangle maps of Venus include similar units; V–9, for example, includes tessera material and densely lineated plains material (units "t" and "prl" of Campbell and Campbell, 2002). Some maps with larger exposures of these deformed materials use geographic subdivisions to categorize outcrops. Although exposures of upland terrain in the Guinevere Planitia quadrangle are not abundant, we subdivided these materials into units t and ul to keep general consistency with other mapping and geomorphologic studies of Venus.

The tectonic features, processes, and evolution of Venus have been extensively studied, and many global and regional analyses have focused on its tesserae (initially called complex ridge terrain) and other highly deformed terrains (Bindschadler and others, 1992; Solomon and others, 1992; Hansen and others, 1997). Tesserae have been interpreted by most researchers as complexly deformed blocks of thickened crust produced by multiple episodes of deformation. Some studies suggest tesserae can be used as a global stratigraphic marker representing the oldest recognizable chronostratigraphic period (Basilevsky and Head 1995a, b; Basilevsky and others, 1997). Other studies propose tesserae result from spatially and temporally distinct tectonic processes in different tectonic environments (Hansen and others, 1997). Although present in the quadrangle, the scarce exposures do not allow rigorous evaluation of the different models for the global geologic evolution of Venus.

Tessera (unit t) exposures within the Guinevere Planitia quadrangle are observed as locally high standing and are always covered by surrounding units. Exposures of lineated upland material (unit ul) are also locally high standing and are observed to include patches of plains along with deformed materials. The local topographic high associated with an exposure of lineated uplands can extend beyond the unit's boundaries to also contain high-standing parts of the surrounding plains. This indicates a complex history of uplift, volcanism, and surface modification.

The tectonic fabric defining each upland terrain exposure (units t and ul) is typically contained within its unit boundaries; however, structural features characteristic of the surrounding unit or units can also be observed within exposures of upland terrain. These features may be entirely contained in the upland

terrain exposure or may extend across the contact between the upland terrain and the surrounding plains or flow materials. Other structural features within the surrounding units terminate at the upland terrain contact. Where lava flows or crater outflows meet upland terrain (or other local topographic highs), the uplands appear to have served as barriers to the flows' advance, or their topography altered flow direction, or both. Three examples include (1) ejecta flows from Seymour crater, which extend around local topographic highs in the regional plains and around an outcrop of tesserae; (2) ejecta flows from Potter crater, which appear to have been deflected by a small volcano; and (3) Atanua Mons' lava flows, which surround Hulda Corona. We interpreted units t, ul, and Var Mons lineated material (unit fVl) within the quadrangle to be locally older materials that were uplifted, tectonically deformed, and superposed by volcanic plains and flows.

Plains Materials

Plains materials dominate the Guinevere Planitia quadrangle in terms of areal extent, occupying 59 percent of the quadrangle (or approximately 4.6×10^6 square kilometers). We divided the extensive volcanic plains materials of the Guinevere Planitia quadrangle into two units on the basis of their general topographic and morphologic characteristics, including the presence, types, and numbers of tectonic and small volcanic features. These units consist of Guinevere lineated and mottled plains (unit pGlm) and Guinevere regional plains (unit pGr). Unit pGlm generally comprises large expanses of rolling topography with a variety of small volcanic cones, domes, shields, and lobate flows (fig. 5). The unit has moderate radar brightness, contains individual radar bright and dark features, and is typically embayed by unit pGr and various types of volcanic flows (fig. 4). However, flows apparently sourced within pGlm also locally superpose unit pGr; these occurrences presumably represent partly visible lobate flow fields that we cannot confidently discriminate with the available radar data.

Tectonic features are common in unit pGlm, and we observed extensional and contractional types, including wrinkle ridges, faults, and troughs. Although tectonic disruption is widespread across the unit, tectonic features exist at a variety of local densities and are commonly concentrated in localized zones. These zones are typically delineated by sets of similar features; for example, groups of wrinkle ridges and faults form both parallel and arcuate patterns. We commonly observed that tectonic features span across contacts between unit pGlm and adjacent plains materials and flow materials units. We also observed faults to be locally buried within unit pGlm. Overall, we interpreted unit pGlm as a composite of areally extensive flows (or multiple smaller flows of similar radar brightness) with many small volcanic edifices and associated lava flows.

Guinevere regional plains (unit pGr) form low-lying regions that are generally radar dark with uniform radar brightness over large distances (fig. 4). Flow margins and small volcanic edifices are evident but not abundant. Wrinkle ridges are the most common type of tectonic feature within unit pGr, and parallel sets of wrinkle ridges are common. Large parts of the unit (for example, near Seymour crater between Atanua and Rhpisunt Montes) have prominent concentrations of densely spaced wrinkle ridges. However, in other large expanses, ridges are rare or exist in substantially lower densities. Individual ridge lengths typically extend to more than 100 km, and ridge sets occur with east-west and northwest-southeast orientations. Faults are also evident; these typically exist in parallel sets and likely indicate local to regional extension. Some faults extend from unit pGr into adjacent flow materials or into unit pGlm. We also observed several canali in unit pGr, including Tingoi Vallis and a feature north of Seymour crater that has branching and braided forms indicative of fluid flow. Other channels display rectilinear patterns. Although its superposition relationships are unclear in some places, unit pGr typically appears to be superposed by all types of volcanic flows, including those associated with the named volcanoes. In several locations, plains-forming flow material (unit fpf) may locally embay unit pGr. Examples include exposures at lat 25° N., long ~307° E., and southwest of Kalm Dorsa at lat ~17.5° N., long 307.5° E.

We interpreted Guinevere regional plains (unit pGr) as volcanic plains comprising areally extensive flows (or multiple smaller flows of similar radar brightness), with local occurrences of small volcanic edifices and flows. Contractional and extensional tectonic features are common, and prominent sets of wrinkle ridges indicate regional deformation. Canali may have served to supply lava to the plains, and the migration of subsurface volatiles may have contributed to the formation of the observed rectilinear network patterns (Baker and others, 1992).

Plains units in Guinevere Planitia are similar to plains units in adjacent quadrangles, and to Venusian plains units in general, both in terms of their radar backscatter characteristics and the types of geologic features contained within the plains units. Copp and Guest (2007), for example, mapped these same two units (units pGlm and pGr) as dominating the Sif Mons quadrangle to the east. Plains are estimated to cover ~70 percent of the Venusian surface, and Guinevere Planitia itself extends for ~7,500 km (Tanaka and others, 1997). They figure prominently into models of the resurfacing history of Venus (Basilevsky and others, 1997; Hansen and others, 1997; Guest and Stofan, 1999) because, in many locations, plains bury tesserae and predate more well-defined lava flow fields, including those associated with volcanoes and coronae.

Flow Materials

Volcanic flow materials are widely observed across the surface of Venus, where they are typically associated with broad shield volcanoes and coronae (Head and others, 1992; Guest and others, 1992; Roberts and others, 1992; Squyres and others, 1992; Stofan and others, 1992, 1997; Crumpler and others, 1997; Smrekar and others, 1997; Tanaka and others, 1997). In an early corona survey, Stofan and others (1992) found that 77 percent of Venusian coronae had moderate to large amounts of associated volcanism. Volcanic flow fields comprise lobate to highly digitate flows that extend from source vents and accumulate in both simple patterns, such as radial flows around central summit vents, and complex patterns, such as intermingled flows from multiple nearby vents. Crumpler and others (1997) identified 1,194 volcanic centers on Venus that are greater than 20 km across and 167 large volcanoes that are greater than 100 km across. They attributed the difference in the formation of a single large edifice versus a field of small edifices to magma production rates, along with the related formation of shallow magma reservoirs.

Various approaches for defining volcanic flow units have been used in the 1:5,000,000-scale quadrangle mapping of Venus (for example, Campbell and Campbell, 2002; Bleamaster and Hansen, 2005; Brian and others, 2005; Copp and Guest, 2007; Lang and Hansen, 2010; Kumar and Head, 2013; McGowan and others, 2019). Units are generally designated as either plains (for example, lobate plains or shield plains) or flow materials. Flow materials are subdivided differently depending on the quadrangle, such as by source morphology or geography. Examples of source-morphology-based names include "corona flow material" or "edifice flow material," whereas geographic names may comprise a feature name (such as a "fluctus," "corona," or "mons") followed by "flow material."

In the Guinevere Planitia quadrangle, we subdivided volcanic flow materials into a series of nine geologic units based on two primary morphologic types and associations with the major named volcanoes. Flow materials consist of plains-forming flow material (unit fpf), lobate flow material (unit fl), which is associated with unnamed sources, and various lobate flow materials associated with named sources (units fA_2, fA_1, fR, fT, fU, fV, and fVl). Outcrops of unit fpf can lack a distinct source and can also be a composite of flow materials from multiple nearby sources (including coronae). Unit fl comprises flow fields associated with smaller, unnamed eruptive centers and flow fields that form the flanks of large, named volcanoes in the map region. Flows associated with named volcanoes were assigned to separate units containing geographic identifiers in their unit names and symbols. This allows for clear delineation of different volcanoes' boundaries and groups the flows with their source vents. This approach, which is commonly used for terrestrial volcanoes and in other maps of Venus, is useful for estimation of magma production and eruption rates.

Plains-forming flow material (unit fpf) comprises extensive, flat-lying sheets that can extend in one or more directions for hundreds of kilometers from their apparent source vents (figs. 6, 7). Unit fpf can be radar bright, moderate, or dark, but radar brightness is typically uniform in any given exposure. The unit is associated with Mehseti Patera and Hulda Corona, and exposures at the latter site are mostly buried by flows from Atanua Mons. Other exposures of unit fpf are adjacent to, and partly buried by, the lobate flows of Uilata Fluctus (unit fU), Tuli Mons (unit fT), Atanua Mons (unit fA_2), and other unnamed volcanic centers.

The largest exposure of unit fpf is in the center of the quadrangle, between Atanua Mons, Var Mons, and Tuli Mons. Here, we identified at least seven quasi-circular features within an expanse of unit fpf. The expanse of unit fpf is embayed by the surrounding volcanoes and likely underlies their distal flanks. Both Madderakka Corona and the large sheet flow extending northeast (named Koti Fluctus) are part of this assemblage (fig. 6). We interpret Madderakka Corona to be the source of Koti Fluctus and propose that the seven quasi-circular features likely produced the mapped flow unit.

Sets of tectonic features, such as wrinkle ridges, broad arches, and faults, intersect unit fpf in the quadrangle. They also delineate quasi-circular volcano-tectonic centers, such as coronae and paterae. The deformation associated with Hulda Corona may extend beyond its associated flow material into unit pGlm to its north and west. Intense deformation, particularly in the large expanse of unit fpf between Atanua and Var Montes, manifests as a high number and density of structural features. These indicate compression (ridges and arches) and extension (faults) in diverse localized circumferential and radial patterns. Another corona-like structure is denoted by arcuate fault patterns in exposures of unit fpf west of Atanua Mons (lat ~13° N., long 303° E.). Here, the faults also extend into adjacent exposures of unit pGlm.

We inferred the emplacement of large sheet flows to have formed unit fpf on the basis of the unit's broadly lobate margins, the lack of substantial relief, and the uniform radar brightness over large distances, although more flow units likely exist than are apparent in the radar images. We interpret unit fpf to represent extensive volcanic flows that erupted primarily from source vents at coronae, corona-like structures, or calderas. Some exposures of this unit have no discernible source vent or have eruptive source areas denoted only by small volcanic constructs.

We found limited ability to discern stratigraphic relationships between exposures of unit fpf in Guinevere Planitia owing to their scattered distribution and a lack of direct contact relationships. In general, however, the unit appears to be locally older than the adjacent exposures of lobate flow material (unit fl), which are associated with named and unnamed volcanic sources. Lobate flow material (unit fl) consists of narrow, sinuous, overlapping deposits with lobate margins that form radial patterns around their source vents (fig. 7). Unit fl can be radar bright, radar dark, or of moderate radar brightness; we observed considerable variations in brightness between adjacent flows from individual vents. Radar brightness within a given flow lobe is commonly uniform, although some lobes show downslope variations in brightness (refer to Byrnes and Crown, 2002). Within the Guinevere Planitia quadrangle, we attribute the formation of the major volcanoes' surfaces to the accumulation of these lobate flows. Where associated with named features, exposures of lobate flow material were mapped separately and with respect to their geographic distribution. This helps delineate the boundaries of the major volcanic centers.

Unit fl is commonly in contact with, and typically superposes, unit fpf. Although tectonic features are present on unit fl, they are substantially less abundant than they are on units fpf, pGr, and pGlm. We observed small volcanic edifices (unit v) and many small domes, cones, and shields (mapped with the "small shield" symbol) in association with unit fl. Many small shields are concentrated in apparent eruptive centers at the summits of lobate flow exposures, or scattered throughout the flow materials, or both.

In addition to lobate flow material units associated with the four named volcanoes and one large flow (Uilata Fluctus), unit fl comprises four smaller, unnamed volcanic centers. One of these, located in the southeast quadrant of the map (east of Var Mons, at lat ~4° N., long 322° E.) is a flow field that lacks a well-defined summit or source area. The second volcanic center consists of two adjacent flow fields, located in the northwest quadrant of the map at lat ~17.5° N., long 303° E., that have merged together to form one exposure of unit fl. Each flow field radiates from a central source area. The source region of the northwest flow field comprises a small volcano (unit v) and a series of small depressions, and the southeast flow field has a central edifice defined by an irregular vent area.

The third unnamed volcanic center, located at lat ~11° N., long 302° E., has flows extending north and south from a chain of volcanic features. These features comprise a concentration of small shields, two steep-sided domes, and a volcanic vent. The flows also encircle a steep-sided dome located slightly to the north. The lobate flows of the fourth unnamed volcanic center form a compound flow field that superposes the eastern flows from the chain of volcanic features. The material of this compound flow field has similarities to Tuli Mons and Uilata Fluctus in terms of its backscatter characteristics, the dimensions of its flow units, and the presence of many small shields on its surface.

In contrast to the lobate flows of the unnamed volcanic centers (unit fl), we categorized the lobate flow materials of the four named volcanoes and one large named flow field into separate units on the basis of their flow patterns and associations with inferred vent or summit regions of the named features. These lobate flow materials are generally similar to unit fl; we note any characteristic differences where present. The first volcano, Rhpisunt Mons, is located in the southwest corner of the Guinevere Planitia quadrangle. Its flanks extend south, southwest, and west into the quadrangles of Navka Planitia (V–42), Phoebe Regio (V–41), and Devana Chasma (V–29), respectively. Rhpisunt Mons rises to ~2,600 m, or ~1,800 m above its surroundings; within the quadrangle, it spans an area of 500 by 650 km. Its summit is defined by two steep-sided domes and a concentric fault pattern that encircles the larger dome (fig. 8). Radial patterns of faults and lava flows extend from Rhpisunt Mons' summit area down its flanks. Lava flows on the distal margins of the volcano superpose the adjacent regional plains. On its east side, lava flows form elongate lobes that extend southeast into an area of plains containing parallel northwest-trending wrinkle ridges.

The flanks of Rhpisunt Mons, mapped as Rhpisunt Mons lobate flow material (unit fR), are, overall, more intensely deformed than those of the other shield volcanoes in the map region. We attribute some of this deformation to Pölöznitsa Corona, located south of Rhpisunt Mons' summit. The patterns of ridges and faults within and to the east of Rhpisunt Mons' south flanks appear to be influenced by the corona; these structural features are arranged in circumferential and radial patterns relative to Pölöznitsa Corona. In addition, the lava flows on the south flank of Rhpisunt Mons are deflected east in response to the topography of the corona.

Var Mons, located along the southern margin of the map region, rises to ~2,450 m, or ~1,700 m above its surroundings. It has a complex summit area denoted by a shield field, a collapsed and embayed steep-sided dome, and a larger irregular dome (fig. 9). The summit flows of Var Mons superpose the upper parts of Nang-byon Chasma, a canyon feature that extends north from the Var Mons summit area. The deformed terrain of Nang-byon Chasma, mapped as a separate flank unit of the volcano (Var Mons lineated material; unit fVl), is locally high standing. It has areas of uniform, moderate radar brightness and areas of bright, dense lineations, with many sets of parallel, linear to arcuate faults. Most of the flanks of Var Mons are mapped as Var Mons lobate flow material (unit fV), which forms an extensive flow field (900 by 1,000 km within the quadrangle) with many lobate flows that extend in a radial pattern around the summit area.

A steep-sided dome on the northwest flanks of Var Mons (the westernmost exposure of two mapped occurrences of the small volcanic edifice unit, discussed in the "Small Volcanoes and Volcanic Features" section) seems to denote a secondary eruptive center on the volcano, which is also indicated by lobate flows that form a radial pattern around it. From variations in radar brightness, we determined that lava flows on the main flanks of Var Mons are wider and longer than those in its summit area or in its secondary eruptive center to the northwest. We attribute this to larger flow volumes for the flank-forming eruptions, and although flow field stratigraphy is likely complex, this may reflect a temporal evolution in eruptive style, with declining eruption rates between the early flank-forming eruptions and the summit eruptions. The lava flows of Var Mons overlie units pGr and fpf to the west, and also overlie unit pGr to the northeast. The south flank of Var Mons is outside the map region in the Navka Planitia quadrangle.

Northwest of Var Mons and to the west of Madderakka Corona and its surrounding flows, expansive flow fields (spanning 950 by 1,100 km) form the flanks of Atanua Mons (fig. 10). Atanua Mons rises to an elevation of ~2,300 m, ~1,700 m above the surrounding terrain. A ~12-km-diameter volcanic cone at its summit is surrounded by lava flows in a radial pattern. The lava flows on the flanks of Atanua Mons vary in brightness, typically widen downslope, and superpose surrounding exposures of other map units (ul, pGlm, pGr, and fpf). Its flanks comprise or contact six small volcanic edifices (unit v), but Atanua Mons is notable within the quadrangle for its lack of small shields and an almost complete absence of structural features.

We subdivided Atanua Mons' flows into two members, determined on the basis of the visible flow patterns, locations relative to the summit and a broad arch on the west flank of the volcano, and their apparent temporal sequence. Atanua Mons lobate flow material, member 1 (unit fA_1) consists of lava flows that form a broad shield in the southwest quadrant of the volcano. These flows are arranged in a radial pattern around Atanua Mons' broad arch, which we interpreted as the margin of an older eruptive center (Brian and others, 2004).

Atanua Mons lobate flow material, member 2 (unit fA_2) consists of lava flows that form a fan-shaped flow field to the west of the summit and a broad shield to the east of the summit. Lava flows of the fan-shaped field combine with an elongate extension of the east field to encircle Hulda Corona, located north of the volcano summit. Hulda Corona itself is defined by a circular exposure of unit ul and interior and exterior exposures of unit fpf; several kīpukas (areas of land surrounded by lava flows) of unit fpf, likely once part of flows associated with Hulda Corona, are evident within unit fA_2 to the east.

Tuli Mons is northeast of Atanua Mons and consists of a large flow field (650 by 650 km) with a summit shield field (fig. 11). Its summit rises ~500 m above its surroundings to an elevation of ~800 m. Exposures of Tuli Mons lobate flow material (unit fT) vary in brightness, and large, bright lobes are more common toward the margins. Variations in radar brightness coupled with the presence of small shields, the latter of which served as topographic obstacles to flow advance, indicate Tuli Mons flows had low viscosities. The flows of unit fT are characterized by branching, elongate shapes and digitate margins.

Northwest of Tuli Mons lies an adjacent flow field referred to as Uilata Fluctus. Lava flows of Uilata Fluctus lobate flow material (unit fU) intermingle with Tuli Mons flows on the south and east sides of the flow field and spread more extensively to the north and northwest, where they form elongate, sinuous lobes. Uilata Fluctus contains many small shields and two large, circular features along its central axis that may be eruptive centers. Its flows vary in brightness, degree of downslope widening, and presence of flow branching. At parts of the Tuli Mons and Uilata Fluctus contact, unit fT clearly superposes unit fU (as indicated by the younger [Y] and older [O] contact labels). The relative age relationships along other parts of the contact are unclear, and some small, locally derived flows of Uilata Fluctus may superpose flows of Tuli Mons.

Small Volcanoes and Volcanic Features

Scattered across the Guinevere Planitia quadrangle are small, locally high-standing, circular to irregular landforms that we mapped as small volcanic edifices (unit v). These are typically 10–30 km in diameter, although they range in diameter from ~5 km to more than 200 km. Individual features can be radar bright, moderate, or dark, typically with little variation across the surface. Some contain lineations on their surfaces and central zones that are elevated or depressed. Their overall profiles can be flat-topped, gently sloping, or steeply sloping from summit to margin. Types of small volcanoes observed in the quadrangle consist of cones, low shields, and steep-sided domes. We interpreted these features as monogenetic volcanoes, and they may consist of accumulations of flow and pyroclastic deposits around an eruptive vent. The features' depressed central zones are interpreted to be a result of subsidence due to lava drainage, but some may be craters formed by small explosive eruptions. Some small volcanic edifices (unit v) are found in summit and other inferred sources regions for volcanic flow materials, including the four named volcanoes. Other small volcanic edifices occur within units pGr and pGlm and in the medial and distal flanks of the named volcanoes.

Steep-sided domes play a significant role in understanding volcanic processes on Venus, given that silicic volcanism has been considered a possible explanation for their distinctive morphology (Guest and others, 1992; Head and others, 1992; McKenzie and others, 1992; Pavri and others, 1992). However, Stofan and others (2000) favored a basaltic composition for steep-sided domes on the basis of their surface characteristics, fracture patterns, and models of crust formation under Venusian conditions. In the Guinevere Planitia quadrangle, we identified 19 steep-sided domes (mapped as exposures of unit v) ranging from ~10 to 70 km in diameter (table 2) (Crown and others, 1993). The domes are circular to highly irregular in planform shape and commonly have pitted, fractured surfaces. Although they feature characteristically steep margins, many domes also have sections with poorly defined edges and can show slumps. Some steep-sided domes have flows extending from them. The modification processes acting on steep-sided domes in the map region are similar to those acting on the surface of Venus in general, with contributions from burial, fracturing, and the collapse of the margins, the interiors, or both (Guest and others, 1992; Pavri and others, 1992; Stofan and others, 2000). Domes in the Guinevere Planitia quadrangle are generally flat-topped, but their surfaces also have variations in relief and may contain pits. Some pits are centrally located on the domes, with concentric fractures indicating formation by collapse. Others have prominent raised rims that may indicate minor secondary eruptive centers, resulting in the accumulation of pyroclastic material on the domes' surfaces.

In the Guinevere Planitia quadrangle, steep-sided domes are found at the summits and on the flanks of the major volcanoes, and in clusters or groups of small edifices within flow fields and on volcanic plains. In some places these groups are composed of different types of small volcanic edifices. Local contact relationships are difficult to assess given the small sizes of steep-sided domes and the complex volcanic environments in which they are found, particularly for those associated with the named volcanoes in the quadrangle. However, several steep-sided domes appear to superpose unit pGr, and in one location (south of Atanua Mons), flows of unit fpf are deflected around the margin of a dome.

Ivanov and Head (1999) conducted a survey of Venusian steep-sided domes in a latitudinal swath centered at lat 30° N. (22.5°–37.5° N.) using once-compressed Magellan mosaicked image data records (C1-MIDRs). Their database comprises 44 steep-sided domes spread across 11 percent of the Venusian surface, 6 of which are in the Guinevere Planitia quadrangle. In contrast, we identified 19 steep-sided domes in the map region (table 2) using F-MAPs. Our list excludes two features identified in the quadrangle by Ivanov and Head because we did not consider them to be steep-sided domes using the full-resolution image mosaics. Ivanov and Head (1999) identified steep-sided domes in a variety of settings, including at the summits of shield volcanoes and in the plains, where the authors describe a close association between the domes and a shield plains unit mapped by other researchers (for example, unit "psh" of Basilevsky, 2008). The distribution they observed across the northern mid-latitudes is generally consistent with the varied distribution we observed across the Guinevere Planitia quadrangle, although typical exposures in V–30 seem to be stratigraphically higher than those found by Ivanov and Head (1999).

We used a variety of map symbols to document the volcanic diversity and history of the Guinevere Planitia quadrangle. "Flow direction" arrows indicate the paths of individual lava flow lobes, making their distribution and patterns within volcanoes or flow units more visible. These patterns are useful in discerning eruptive vent locations and sequences of flow emplacement. We also used flow direction arrows to document the properties of crater ejecta outflows (for example, lobes associated with Potter and Seymour craters).

The "small depression" symbol is used to mark the locations of small depressions, which range in diameter from ~1 km to ~10 km. These depressions are found on the surfaces of small volcanic edifices (unit v), are scattered throughout the quadrangle, and commonly occur near small shields. Although we interpret these as likely volcanic collapse craters, we acknowledge they are too small to be definitively described with available image mosaics.

"Small shields," which are ~5 to ~15 km in diameter, are hills with a difference in radar brightness from their surroundings, hills with a small summit depression, or both. We interpreted small shields to be monogenetic volcanic features too small to

Table 2. Steep-sided domes in the Guinevere Planitia quadrangle.

[Some irregularly shaped features described with measurements of two axes. ° N., degrees north; ° E., degrees east; km, kilometers; fR, Rhpisunt Mons lobate flow material; fV, Var Mons lobate flow material; —, no data; pGr, Guinevere regional plains; fpf, plains-forming flow material; fVl, Var Mons lineated material; fA1, Atanua Mons lobate flow material, member 1; fA2, Atanua Mons lobate flow material, member 2; fl, lobate flow material; pGlm, Guinevere lineated and mottled plains]

Latitude (° N.)	Longitude (° E.)	Diameter or major and minor axes (km)	Dome morphology	Surface features	Volcanic associations	Contacts with units
0.0	302.2	15.9	Irregular	Summit pit	Corona center	fR
1.6	316.1	24.3	Irregular	Summit pit	Volcano summit	fV
2.6	314.1	25.8	Circular	—	Volcano flank	fV
2.7	301.3	10.8	Irregular	Pit with rim	Volcano summit	fR
3.6	309.3	58.1	Circular	Summit pit	Cluster in plains	pGr, fpf
4.3	315.7	23.8	Irregular	Pit with rim	Volcano flank	fVl
7.4	305.5	10.8	Circular	Fractures	Volcano flank	fA_1
7.8	311.0	35.8	Irregular	Fractures	Volcano flank	fA_2
10.1	302.1	31.0 by 71.6	Irregular	Fractures; pits	Cluster	pGr, fl
10.3	301.0	17.6	Irregular	Summit pit	Cluster	fl
10.8	313.4	11.9	Irregular	—	Group	fpf
11.0	301.5	31.1	Circular	Fractures	Cluster	fl
11.0	313.4	11.9	Circular	Pit with rim	Group	fpf
12.3	316.4	15.9 by 19.9	Irregular	Fractures	Plains	fpf
14.1	303.0	15.9	Circular	—	Corona?	pGlm
23.1	319.4	11.9	Circular	Summit pit; fractures	Plains	pGlm
24.4	314.1	19.9	Irregular	Summit pit; fractures	Corona margin	pGlm
24.7	314.3	17.9	Circular	Pit with rim	Corona margin	pGlm
25.0	314.0	15.9 by 31.8	Irregular	Pit with rim	Corona margin	pGlm

adequately characterize in Magellan radar images. These features are scattered across the quadrangle at a variety of densities, from isolated features to small groups to large concentrations. They are found in every map unit and some are associated with lava flow fields. High concentrations of small shields were observed at the summits of Tuli and Var Montes and within Uilata Fluctus. They are abundant in northern exposures of unit pGlm, but less abundant in other exposures of the unit. In some geologic maps of Venus, map authors used high concentrations of small shields to identify and define one or more distinct geologic map units; for example, "shield plains material" (Brian and others, 2005; Basilevsky, 2008; Kumar and Head, 2013), "edifice field material" (Brian and others, 2005; Copp and Guest, 2007), and "shield flow material" (Bleamaster and Hansen, 2005). In other geologic maps of Venus, authors map shields solely as point features within a particular unit (Campbell and Campbell, 2002) or as a prominent characteristic of a particular unit, similar to our unit pGlm (that is, "shield terrain" in Lang and Hansen, 2010). In the geologic mapping of the region spanning lat 0–25° N. and long 90–150° E., Hansen (2005) described widespread shield terrain and small shields with densities ranging from 3,500 to 33,500 shields per million square kilometers.

Channels

We observed channels at several locations within the Guinevere Planitia quadrangle, although they occur predominantly in unit pGr (figs. 4, 8, 9). These channels are interpreted to be volcanic in origin. They have linear to curvilinear forms and are found both individually and in small networks. Singular channels typically have low sinuosity, whereas Tingoi Vallis (northeast of Var Mons) is characterized by an anastomosing pattern. All the channel networks observed in the map region are simple systems without higher-order tributaries. This, along with a lack of apparent development beyond incipient dendritic and rectilinear patterns, indicates they are not mature systems. We attribute one example, a channel network within unit pGr east of Rhpisunt Mons, to the migration of subsurface volatiles, as suggested by Baker and others (1992, 1997). In this location, we mapped a series of small, high-angle tributaries arranged in a rectilinear pattern (fig. 8). The main channel and its tributaries all show scalloped margins consistent with parts of the adjacent plains. We inferred an overall transport direction of northwest to southeast in this network, determined from the directions of main channel narrowing and decreasing tributary length.

Impact Craters

We mapped nine impact craters in the Guinevere Planitia quadrangle (table 1). The deposits associated with these impact craters, including their rims, ejecta blankets, central peaks, and ejecta outflow deposits (if present) are mapped as impact crater material (unit c). An additional map symbol is used to denote the crests of crater rims. Most crater materials are radar bright, but radar dark deposits commonly dominate their floors. These dark crater floors, which are common on the surface of Venus, presumably reflect the modification or infilling of the initial fresh, radar bright crater interior (Schaber and others, 1992). Within six impact craters, we observed radar bright hills or mounds; these may represent central peaks or remnants of central peaks. Seymour and Potter craters have ejecta outflows; these elongate, sinuous lobate flows extend from the edges of crater ejecta blankets onto adjacent terrain, reaching distances of 100 km or more. Many researchers have interpreted Venusian crater outflows as thin ejecta materials made of a mixture of gases and melt, whose emplacement was influenced by the local surface topography (Asimow and Wood, 1992; Schaber and others, 1992; Herrick and others, 1997; McKinnon and others, 1997). Radar brightness patterns within the crater rims suggest terracing in some craters, such as Shih Mai-Yu and Caroline. Stipple-patterned symbology on the map denotes bright halos and dark halos associated with impact craters (refer to Campbell and others, 1992; Schultz, 1992). Halos in the quadrangle have a wide variety of sizes and are quasi-circular to slightly elongate in shape.

Structural Features

Structural features exist across the Guinevere Planitia quadrangle but are in greatest abundance (1) in units pGr and pGlm, (2) in association with coronae and corona-like circular structures, (3) within some volcanic flow fields, and (4) as characteristic components of highly deformed upland terrain. We identified and mapped a variety of structural feature types, including wrinkle ridges, broad arches, faults, and troughs. However, not all structural features can be feasibly mapped at the 1:5,000,000 scale, so the map sheet does not include comprehensive documentation of all structural features in the quadrangle. Instead, it describes the diversity of identified feature types and the representative distributions, orientations, and densities of the main structural features.

The wrinkle ridges observed in the Guinevere Planitia quadrangle are curved or arcuate and are identified by the radar bright signatures of their narrow, crenulated ridge crests. They are commonly interpreted as contractional tectonic features, with their deformation a reflection of surface shortening caused by compressional stresses. Broad arches are arcuate features with noticeable topographic expression also resulting from compressional stresses. These delineate eruptive centers within the named volcanoes and the large exposure of unit fpf between Atanua and Var Montes. They also occur along with dense sets of other structural features in units ul and fVl.

Faults in the quadrangle are linear to arcuate and are primarily extensional in nature, as indicated by negative relief in Magellan image mosaics. They are typically narrow and have a wide variety of lengths, with some individual features reaching several hundred kilometers long. Although many mapped faults show clear negative relief, the morphology of others is poorly expressed in SAR mosaics.

Troughs, like faults, are also linear to arcuate features but are wider, shorter, have greater sinuosity, and commonly vary in width and morphology along their lengths. Some troughs or trough segments occur as pit chains. Troughs are substantially less abundant than faults and occur near near small eruptive centers at radial and circumferential orientations, and in small groups within the plains.

Wrinkle ridges and faults are the most common structural features in the Guinevere Planitia quadrangle and are common in units pGr and pGlm. Given their abundance and the large areal extents of those units, wrinkle ridges and faults may be indicators of regional structural evolution. However, their distribution and orientations do not indicate a dominant tectonic fabric at the scale of the quadrangle.

In the extensive plains units that dominate the east part of the quadrangle, many wrinkle ridges trend east-west to northwest-southeast. We observed similar wrinkle ridge trends in the plains units of the northwestern and southwestern parts of the quadrangle. However, in the northwestern and southeastern parts of the quadrangle, fault sets in unit pGr trend north-south to northwest-southeast. The structural features of unit pGr exist in various densities and orientations but are mostly found in sets of similarly trending features.

Unit pGlm also contains wrinkle ridges and faults, although it has more abundant faults and fault sets than unit pGr. In some locations, structural patterns (as well as some individual structural features) extend across contacts between the plains units; in other locations, sets of structural features are confined to a single unit. The overall distribution and variations in density of wrinkle ridges and faults indicate a history of varied stress regimes at local and regional scales, which over time produced the complex and diverse patterns now present in the region. The larger-scale, more consistent patterns of wrinkle ridges that deform unit pGr might, in part, be attributed to a more homogeneous substrate within the unit relative to that of unit pGlm.

Structural features are also present within, or in association with, flow materials. Patterns of such features indicate more localized responses or discrete stress regimes compared to those observed in the plains materials. One prominent deformation zone, Nang-byon Chasma, extends 250 km north from the summit of Var Mons and features densely spaced faults, a series of broad arches, and several wrinkle ridges. In the central part of the map region, sets of densely spaced wrinkle ridges and faults surround Madderakka Corona and adjacent corona-like structures, oriented in radial and circumferential patterns. Other distinctive fault sets exist on Rhpisunt Mons (arranged in a radial pattern), within unit pGlm north of Hulda Corona (also in a radial pattern), and extending through and beyond Uilata Fluctus (trending north-south in a parallel arrangement). Similar to the plains materials, volcano-associated ridge and fault sets are typically confined to a single geologic unit (for example, the fractures on Rhpisunt Mons). However, some instances do cross unit contacts, such as the faults between unit fU and unit pGlm to the north. Some other individual features are truncated along unit contacts.

Geologic History

The geologic mapping of Venus' Guinevere Planitia quadrangle provided valuable constraints for determining the geologic history of its landscape. These constraints include stratigraphic and cross-cutting relationships observed or inferred from analyses of Magellan datasets. Relationships were documented through the definition of map units, unit boundaries, and geologic features. Specific relationships between geologic units are presented in table 3. The "Correlation of Map Units" section (refer to map sheet) shows a quadrangle-scale synthesis of the relative temporal extents of, and relationships between, map units.

Mapped geologic units in the quadrangle show a general age progression, determined on the basis of the most commonly observed stratigraphic relationships. The upland terrain units are older than the plains materials, which in turn are older than the flow materials, small volcanoes, and impact craters. This progression has been described in other studies of Venus (Basilevsky and others, 1997; see also Tanaka and others [1997] for a synthesis), including in 1:5,000,000-scale geologic maps (for example, adjacent maps by Copp and Guest [2007] and McGowan and others [2019]). Repeated patterns of these major geologic units are observed in other regions of Venus. Coupled with interpretations of crater densities, these patterns have been used to suggest a global stratigraphic record and global synchroneity of major geologic events—for example, tessera formation (Basilevsky and others, 1997). In a synthesis of tectonism on Venus, Hansen and others (1997) concluded that its major tectonic processes are either cyclic or evolutionary and produce diachronous geologic patterns. They formulated a vertical tectonic model in which plains formed in regions of broad mantle downwelling, with subsequent tectonic and magmatic resurfacing at regional and local scales. Guest and Stofan (1999) interpreted the surface of Venus as the result of a nondirectional geologic history, with repeated patterns of events occurring in different places at different times throughout its past.

This 1:5,000,000-scale geologic map of part of Guinevere Planitia documents its surface geology and stratigraphy to derive the geologic history of the Guinevere Planitia quadrangle, and it

Table 3. Stratigraphic relationships between geologic units and features in the Guinevere Planitia quadrangle.

[Only features and units in direct contact are compared to one another. Some unit relationships are uncertain, for example, gradational relationships or conflicting embayment relationships produced by local topography. Where a relationship with unit c involves a specific crater, the crater name is given in parentheses. This provides additional stratigraphic information where relative ages are distinct between individual craters and adjacent units. Locally, craters may have clear superposition or cross-cutting relationships with adjacent units, but impact craters have different ages across the region, and given the complex histories of volcanism and plains emplacement, local age relationships are not always clear. t, tessera; pGlm, Guinevere lineated and mottled plains; pGr, Guinevere regional plains; fpf, plains-forming flow material; ul, lineated upland material; fA2, Atanua Mons lobate flow material, member 2; fA1, Atanua Mons lobate flow material, member 1; fT, Tuli Mons lobate flow material; fl, lobate flow material; fV, Var Mons lobate flow material; v, small volcanic edifice; fU, Uilata Fluctus lobate flow material; fR, Rhpisunt Mons lobate flow material; fVl, Var Mons lineated material; c, impact crater material; —, not applicable]

Unit	Younger Than	Overlaps With	Older Than	Uncertain
t	—	—	pGlm, pGr, fpf, c(Seymour)	—
ul	—	—	pGlm, pGr, fA_2, fA_1, fT, fl, fpf	pGlm, pGr
pGlm	t, ul	pGr, fpf	fA_2, fV, fT, fR, v, fl, fpf, c(Shih Mai-Yu)	ul, v
pGr	t, ul	pGlm	fA_2, fA_1, fV, fT, fU, fR, fl, fpf, c(Gundrun, Seymour)	ul, fpf, v
fA_2	ul, pGlm, fA_1, fpf, v	c(Potter)	—	v, fl
fA_1	ul, pGr, v	—	fA_2, c(Caroline)	—
fV	pGlm, pGr, fpf	fVl, v	c(Kala)	fl
fVl	—	fV, v	pGr, fpf	—
fT	ul, pGlm, pGr, fpf	fU	—	—
fU	pGlm, pGr, fpf	fT	c(Neda, Vard)	—
fR	pGlm, pGr	c(Ketzia)	—	v
v	pGlm, pGr	fV, fVl	fA_2, fA_1, fpf, c(Potter)	pGlm, pGr, fA_2, fR, fl
fl	ul, pGlm, pGr, fpf	—	—	fA2, fV, v
fpf	t, ul, pGlm, pGr, v	pGlm	fA_2, fV, fT, fl	—
c	pGlm, pGr, fA_1, fV, fT, v	fA2, fR	—	—
Small shields	All units	—	c(Seymour)	—
Small depressions	pGlm, fV, fl, fpf, v	—	—	—
Haloes	t, ul, pGlm, pGr, fA_2, fA_1, fV, fT, fl, fpf, c, v	—	—	—
Canali	pGr	—	—	—

also allows for comparisons to current and future global models for Venus. Although geologic patterns common to other regions of Venus are evident in the Guinevere Planitia quadrangle, local relative ages are inconsistent or unclear. This prevents robust stratigraphic correlation across the quadrangle. The mapping results do suggest complicated local sequences of volcanic and tectonic activity, but it is not clear whether the commonly observed local geologic patterns occurred contemporaneously across the quadrangle.

Geologic analyses of Laufey Regio from Magellan data, by Brian and others (2004) and by this formal geologic mapping investigation, have produced largely consistent results, although with some differences. Brian and others (2004) used Magellan F-MAPs to identify and describe geologic units associated with Atanua, Tuli, and Var Montes, along with units in the surrounding terrain. These analyses, which also included geophysical studies, suggested that Laufey Regio is a volcano-dominated rise in a late evolutionary stage. They also subdivided plains and flow materials but did so using more units than in this investigation. Key results of their work included evidence for (1) protracted evolution of the large volcanic centers with multiple summit sources in addition to flank vents, and (2) temporal overlap between the formation of coronae and volcanoes. Each of these are consistent with a nondirectional geologic history (for more information, refer to Guest and Stofan, 1999).

Detailed geologic (tectonic and volcanic) observations and patterns have been documented through this geologic mapping investigation of the Guinevere Planitia quadrangle. Upland terrains, preserved as embayed remnants and typically found within plains materials, show intense tectonic deformation and uplift. Uplift, however, is not confined to the upland terrain, but also affects both the upland terrain and parts of the surrounding Guinevere plains (units pGr and pGlm). In addition, patches of plains too small to map at a 1:5,000,000 scale were observed within outcrops of upland terrain (units ul and t), further indicating the geologic complexity of upland terrain despite its relatively scarce exposure in the map region relative to other mapped units.

Tectonic features, primarily wrinkle ridges and faults, are abundant in the Guinevere Planitia quadrangle. They are more abundant in older units, such as upland terrain and plains materials, and less common in flow materials, particularly in certain exposures of lobate flow material (such as units fA_1, fA_2, and fT). The tectonic features of the map region commonly occur in sets, indicating deformation at a localized rather than regional scale. Although some features are concentrated in, and characteristic of, certain units (for example, wrinkle ridges in unit pGr), tectonic features show inconsistent relationships with unit boundaries; they are not typically confined to a single unit and commonly cross geologic contacts. These observations support the view of tectonic features as secondary characteristics of geologic units and indicate complicated temporal sequences of deformation throughout the units' formation.

The density of tectonic features in different parts of the quadrangle may act as an indicator of relative age, where a dearth of features indicates younger material. If this is correct, Atanua Mons, Tuli Mons, and the unit fl flow fields at lat ~17.5° N., long 303° E. and lat ~11° N., long 303° E. may be the sites of the most recent eruptive activity in the map region. We observed sets of wrinkle ridges crossing the distal contacts of Atanua Mons (to its west), Rhpisunt Mons (to its east), and Var Mons (to its northeast). Additionally, flows on Atanua and Rhpisunt Montes are deflected by ridges. These relationships indicate that in these areas, Guinevere regional plains formed first, followed by wrinkle ridges and then lava flows.

Local superposition relationships and variations in radar brightness indicate that units pGr, pGlm, and fpf seem to be assemblages of volcanic flows emplaced from multiple sources, including from distinct coronae and corona-like structures. The radar brightness and morphology of these units indicate that large volcanic flows may have produced exposures of units pGr and fpf. Exposures of unit pGlm, in contrast, feature many local centers of volcanic and tectonic activity, which we attributed to a more complicated formation history for that unit. Structural features found in unit pGlm include many sets of ridges and faults, features that may be associated with coronae or corona-like structures, and many small volcanic features, including small shields, depressions, and other volcanic edifices. Some small volcanic features in unit pGlm appear to have small, related flow lobes, but flow lobes with no apparent source vents were also observed. The temporal evolution of unit pGlm remains unresolved, but was likely protracted, with a continued production of small volcanic edifices over a long period.

The morphologic and radar brightness characteristics of volcanoes in the quadrangle indicate that their volcanic evolution may involve (1) multiple large-scale eruptive centers with recognizable spatial and temporal sequences, (2) extensive lava flow fields with a multitude of flows arranged in complex overlapping patterns, and (3) many small volcanic edifices, including shields, domes, and cones. These observations indicate significant variation in eruptive styles within a given mapped volcano and are consistent with complicated sequences of volcanic activity.

Rhpisunt and Tuli Montes have centralized summit source areas; Rhpisunt Mons' summit has several small volcanoes and Tuli Mons' summit has a concentration of small shields. Atanua and Var Montes have compound source areas, with clear evidence at Atanua Mons for a temporal evolution from one source area to another. Uilata Fluctus also has a compound or distributed source area. All five of these major volcanic centers have small volcanoes, small shields, or both at their summits or at other inferred source areas. The four large volcanoes appear to record waning long-term eruption rates, with distal zones that typically have longer, larger flow lobes than those of the upper flank and summit areas (which also contain shield fields, cones, and domes). These small volcanic edifices, which are intermingled with lobate lava flows, indicate smaller eruption volumes from both distributed eruptive vents and shield volcano summits. These edifices, which also form clusters or chains within unnamed flow fields, indicate variation in eruption rates, eruptive styles, or both. We interpreted cones to be a result of minor pyroclastic activity, whereas steep-sided domes were attributed to a distinct relationship between lava supply and cooling history. The identification of large-scale volcanic units (plains, flow fields, and shield volcanoes), volcanic source areas (coronae and large-scale vents within shield volcanoes), and eruptive product patterns indicate the presence of long-lived eruptive centers within

Guinevere Planitia. In addition, the size, number, and distribution of exposures of unit fpf indicate that what were once extensive units may now only exist as smaller exposures, a result of their partial burial by the younger, lobate flows. Plains-forming flows (unit fpf) may represent an early phase of central vent volcanism, with flows sourced at coronae or corona-like structures prior to a shield-building phase. The potential evolution from widespread plains to shield volcanoes concurrently across the quadrangle is consistent with, but not directly supported by, the observed stratigraphy. The volcanic morphologies and the diversity of landforms identified in this study do not require evolved magmas and can be reasonably interpreted as a result of basaltic volcanism. We attribute the different observed morphologies (plains, flows, and small volcanic edifices) to the differences in supply conditions, emplacement rates, cooling history, or all of the above, that may have occurred across Guinevere Planitia over time.

Acknowledgments

The authors thank Jeff Plaut for science discussions in the early phases of this investigation and Marc Hunter and Dan Berman for technical assistance. This research was funded by NASA grants from the Venus Data Analysis Program (to E.R. Stofan) and the Planetary Geology and Geophysics Program (to L.F. Bleamaster III).

References Cited

Anderson, S.W., Stofan, E.R., Plaut, J.J., and Crown, D.A., 1998, Block size distributions on silicic lava flow surfaces—Implications for emplacement conditions: Geological Society of America Bulletin, v. 110, no. 10, p. 1258–1267, https://doi.org/10.1130/0016-7606(1998)110<1258:BSDOSL>2.3.CO;2.

Arvidson, R.E., Plaut, J.J., Jurgens, R.F., Saunders, R.S., and Slade, M.A., 1990, Geology of southern Guinevere Planitia, Venus, based on analyses of Goldstone radar data, *in* Sharpton, V.L. and Graham, R., eds., Proceedings of the Twentieth Lunar and Planetary Science Conference, Houston, Tex., March 13–17, 1989: Houston, Tex., Lunar and Planetary Institute, p. 557–572.

Asimow, P.D., and Wood, J.A., 1992, Fluid outflows from Venus impact craters—Analysis from Magellan data: Journal of Geophysical Research, v. 97, no. E8, p. 13643–13666, https://doi.org/10.1029/92JE00981.

Baker, V.R., Komatsu, G., Parker, T.J., Gulick, V.C., Kargel, J.S., and Lewis, J.S., 1992, Channels and valleys on Venus—Preliminary analysis of Magellan data: Journal of Geophysical Research, v. 97, no. E8, p. 13421–13444, https://doi.org/10.1029/92JE00927.

Baker, V.R., Komatsu, G., Gulick, V.C., and Parker, T.J., 1997, Channels and valleys, *in* Bougher, S.W., Hunten, D.M., and Phillips, R.J., eds., Venus II—Geology, geophysics, atmosphere, and solar wind environment: Tucson, Ariz., University of Arizona Press, p. 757–793.

Basilevsky, A., Head, J.W., III, Schaber, G.G., and Strom, R.G., 1997, The resurfacing history of Venus, *in* Bougher, S.W., Hunten, D.M., and Phillips, R.J., eds., Venus II—Geology, geophysics, atmosphere, and solar wind environment: Tucson, Ariz., University of Arizona Press, p. 1047–1084.

Basilevsky, A., 2008, Geologic map of the Beta Regio Quadrangle (V–17), Venus: U.S. Geological Survey Scientific Investigations Map 3023, 1 sheet, scale 1:5,000,000, 34-p. pamphlet, https://doi.org/10.3133/sim3023.

Basilevsky, A., and Head, J.W., III, 1995a, Global stratigraphy of Venus—Analysis of a random sample of thirty-six test areas: Earth, Moon, and Planets, v. 66, p. 285–336, https://doi.org/10.1007/BF00579467.

Basilevsky, A., and Head, J.W., III, 1995b, Regional and global stratigraphy of Venus—A preliminary assessment and implications for the geological history of Venus: Planetary and Space Science, v. 43, no. 12, p. 1523–1553, https://doi.org/10.1016/0032-0633(95)00070-4.

Bindschadler, D.L., deCharon, A., Beratan, K.K., Smrekar, S.E., and Head, J.W., III, 1992, Magellan observations of Alpha Regio—Implications for formation of complex ridged terrains on Venus: Journal of Geophysical Research, v. 97, no. E8, p. 13563–13578, https://doi.org/10.1029/92JE01332.

Bleamaster, L.F., III, and Hansen, V.L., 2005, Geologic map of the Ovda Regio Quadrangle (V–35), Venus: U.S. Geological Survey Geologic Investigations Map I-2808, 1 sheet, scale 1:5,000,000, 13-p. pamphlet, https://doi.org/10.3133/i2808.

Brian, A.W., Stofan, E.R., and Guest, J.E., 2005, Geologic map of the Taussig Quadrangle (V–39), Venus: U.S. Geological Survey Scientific Investigations Map 2813, 1 sheet, scale 1:5,000,000, 20-p. pamphlet, https://doi.org/10.3133/sim2813.

Brian, A.W., Stofan, E.R., Guest, J.E., and Smrekar, S.E., 2004, Laufey Regio—A newly discovered topographic rise on Venus: Journal of Geophysical Research, v. 109, no. E7, article E07002, https://doi.org/10.1029/2002JE002010.

Byrnes, J.M., and Crown, D.A., 2002, Morphology, stratigraphy, and surface roughness properties of Venusian lava flow fields: Journal of Geophysical Research, v. 107, no. E10, article 5079, https://doi.org/10.1029/2001JE001828.

Campbell, B.A., 1995, Use and presentation of Magellan quantitative data in Venus mapping: U.S. Geological Survey Open File Report 95-519, 27 p., https://doi.org/10.3133/ofr95519.

Campbell, B.A., Arvidson, R.E., and Shepard, M.K., 1993, Radar polarization of volcanic and playa surfaces—Applications to terrestrial remote sensing and Venus data interpretation: Journal of Geophysical Research, v. 98, no. E9, p. 17099–17113, https://doi.org/10.1029/93JE01541.

Campbell, B.A., and Campbell, D.B., 1992, Analysis of volcanic surface morphology on Venus from comparison of Arecibo, Magellan, and terrestrial airborne radar data: Journal of Geophysical Research, v. 97, no. E10, p. 16293–16314, https://doi.org/10.1029/92JE01558.

Campbell, B.A., and Campbell, P.G., 2002, Geologic map of the Bell Regio Quadrangle (V–9), Venus: U.S. Geological Survey Geologic Investigations Map I-2743, 1 sheet, scale 1:5,000,000, https://doi.org/10.3133/i2743.

Campbell, D.B., Head, J.W., III, Senske, D.A., Fisher, P.C., Hine, A.A., and Harmon, J.A., 1989, Styles of volcanism on Venus—New Arecibo high resolution radar data: Science, v. 246, no. 4928, p. 373–377, https://doi.org/10.1126/science.246.4928.373.

Campbell, B.A., and Rogers, P.G., 1994, Bell Regio, Venus—Integration of remote sensing data and terrestrial analogs for geologic analysis: Journal of Geophysical Research, v. 99, no. E10, p. 21153–21171, https://doi.org/10.1029/94JE01862.

Campbell, D.B., Stacy, N.J.S., Newman, W.I., Arvidson, R.E., Jones, E.M., Musser, G.S., Roper, A.Y., and Schaller, C., 1992, Magellan observations of extended impact crater related features on the surface of Venus: Journal of Geophysical Research, v. 97, no. E10, p. 16249–16278, https://doi.org/10.1029/92JE01634.

Copp, D.L., and Guest, J.E., 2007, Geologic map of the Sif Mons Quadrangle (V–31), Venus: U.S. Geological Survey Scientific Investigations Map 2898, 1 sheet, scale 1:5,000,000, https://doi.org/10.3133/sim2898.

Crown, D.A., and Stofan, E.R., 2006, Geologic mapping of the Guinevere Planitia Quadrangle of Venus, *in* Abstracts of the Annual Meeting of Planetary Geologic Mappers, Nampa, Idaho, 2006: U.S. Geological Survey Open-File Report 2006-1263, 54 p., https://doi.org/10.3133/ofr20061263.

Crown, D.A., Stofan, E.R., and Bleamaster, L.F., III, 2008a, Geologic mapping of the Guinevere Planitia Quadrangle (V–30) of Venus [abs.], *in* 39th Lunar and Planetary Science Conference, League City, Tex., March 14–18, 2008, Abstracts: Lunar and Planetary Science Conference, abstract 1725.

Crown, D.A., Stofan, E.R., and Bleamaster, L.F., III, 2008b, Geologic mapping of the Guinevere Planitia Quadrangle of Venus, *in* Bleamaster, L.F., III, Tanaka, K.L, Kelley, M.S., eds, Abstracts of the Annual Meeting of Planetary Geologic Mappers, Flagstaff, Ariz., June 23–26, 2008: Washington D.C., NASA Conference Publication CP-2008-215469.

Crown, D.A., Stofan, E.R., and Bleamaster, L.F., III, 2011, Geologic map of the Guinevere Planitia quadrangle of Venus [abs.], *in* 42nd Lunar and Planetary Science Conference, The Woodlands, Tex., March 7–11, 2011, Abstracts: Lunar and Planetary Science Conference, abstract 1448.

Crown, D.A., Stofan, E.R., and Plaut, J.J., 1993, Volcanism in southern Guinevere Planitia, Venus—Regional volcanic history and morphology of volcanic domes [abs.], *in* 24th Lunar and Planetary Science Conference, Houston, Tex., March 15–19, 1993, Abstracts: Lunar and Planetary Science Conference, abstract 1179, p. 355–356.

Crown, D.A., Stofan, E.R., and Plaut, J.J., 1994, Geology of the Guinevere Planitia quadrangle of Venus [abs.], *in* 25th Lunar and Planetary Science Conference, Houston, Tex., March 14–18, 1994, Abstracts: Lunar and Planetary Conference abstract 1151, p. 301–302.

Crumpler, L.S., Aubele, J.C., Senske, D.A., Keddie, S.T., Magee, K.P., and Head, J.W., 1997, Volcanoes and centers of volcanism on Venus, *in* Bougher, S.W., Hunten, D.M., and Phillips, R.J., eds., Venus II—Geology, geophysics, atmosphere, and solar wind environment: Tucson, Ariz., University of Arizona Press, p. 697–756.

Ford, J.P., Plaut, J.J., Weitz, C.M., Farr, T.G., Senske, D.A., Stofan, E.R., Michaels, G., and Parker, T.J., 1993, Guide to Magellan image interpretation: Pasadena, Calif., California Institute of Technology, Jet Propulsion Laboratory Publication 93-24, NASA Contractor Report CR-194340, 148 p.

Guest, J.E., Bulmer, M.H., Aubele, J., Beratan, K., Greeley, R., Head, J.W., III, Michaels, G., Weitz, C., and Wiles, C., 1992, Small volcanic edifices and volcanism in the plains of Venus: Journal of Geophysical Research, v. 97, no. E10, p. 15949–15966, https://doi.org/10.1029/92JE01438.

Guest, J.E., and Stofan, E.R., 1999, A new view of the stratigraphic history of Venus: Icarus, v. 139, no. 1, p. 55–66, https://doi.org/10.1006/icar.1999.6091.

Hagfors, T., 1964, Backscattering from an undulating surface with applications to radar returns from the Moon: Journal of Geophysical Research, v. 69, no. 18, https://doi.org/10.1029/JZ069i018p03779.

Hansen, V.L., 2005, Venus's shield terrain: Geological Society of America Bulletin, v. 117, no. 5-6, p. 808–822, https://doi.org/10.1130/B256060.1.

Hansen, V.L., Willis, J.J., and Banerdt, W.B., 1997, Tectonic overview and synthesis, *in* Bougher, S.W., Hunten, D.M., and Phillips, R.J., eds., Venus II—Geology, geophysics, atmosphere, and solar wind environment: Tucson, Ariz., University of Arizona Press, p. 797–844.

Hansen, W.R., ed., 1991, Suggestions to authors of the reports of the United States Geological Survey (7th ed.): Reston, Va., U.S. Geological Survey, 289 p., https://doi.org/10.3133/7000088.

Head, J.W., III, Crumpler, L.S., Aubele, J.C., Guest, J.E., and Saunders, R.S., 1992, Venus volcanism—Classification of volcanic features and structures, associations, and global distribution from Magellan data: Journal of Geophysical Research, v. 97, no. E8, p. 13153–13197, https://doi.org/10.1029/92JE01273.

Head, J.W., III, and Wilson, L., 1986, Volcanic processes and landforms on Venus—Theory, predictions, and observations: Journal of Geophysical Research, v. 91, no. B9, p. 9407–9446, https://doi.org/10.1029/JB091iB09p09407.

Herrick, R.R., Sharpton, V.L., Malin, M.C., and Lyons, S.N., 1997, Morphology and morphometry of impact craters, *in* Bougher, S.W., Hunten, D.M., and Phillips, R.J., eds., Venus II—Geology, geophysics, atmosphere, and solar wind environment: Tucson, Ariz., University of Arizona Press, p. 1015–1046.

Ivanov, M.A., and Head, J.W., III, 1999, Stratigraphic and geographic distribution of steep-sided domes on Venus—Preliminary results from regional geologic mapping and implications for their origin: Journal of Geophysical Research, v. 104, no. E8, p. 18907–18924 https://doi.org/10.1029/1999JE001039.

Klose, K.B., Wood, J.A., and Hashimoto, A., 1992, Mineral equilibria and the high radar reflectivity of Venus mountaintops: Journal of Geophysical Research, v. 97, no. E10, p. 16353–16370, https://doi.org/10.1029/92JE01865.

Kumar, P.S., and Head, J.W., III, 2013, Geologic map of the Lada Terra quadrangle (V–56), Venus: U.S. Geological Survey Scientific Investigations Map 3249, 1 sheet, scale 1:5,000,000, 11-p. pamphlet, https://doi.org/10.3133/sim3249.

Lang, N.P., and Hansen, V.L., 2010, Geologic map of the Greenaway quadrangle (V–24), Venus: U.S. Geological Survey Scientific Investigations Map 3089, 1 sheet, scale 1:5,000,000, 15-p. pamphlet, https://doi.org/10.3133/sim3089.

McGowan, E.M., Buczkowski, D.L., and McGill, G.E., 2019, The Lachesis Tessera quadrangle (V–18), Venus [abs.], *in* 50th Lunar

and Planetary Science Conference, The Woodlands, Tex., March 18–22, 2019, Abstracts: Lunar and Planetary Science Conference, LPI Contribution no. 2132, Abstract 1303.
McKenzie, D., Ford, P.G., Liu, F., and Pettengill, G.H., 1992, Pancake-like domes on Venus: Journal of Geophysical Research, v. 97, no. E10, p. 15967–15976, https://doi.org/10.1029/92JE01349.
McKinnon, W.B., Zahnle, K.J., Ivanov, B.A., and Melosh, H.J., 1997, Cratering on Venus—Models and observations, *in* Bougher, S.W., Hunten, D.M., and Phillips, R.J., eds., Venus II—geology, geophysics, atmosphere, and solar wind environment: Tucson, Ariz., University of Arizona Press, p. 969–1014.
Pavri, B., Head, J.W., III, Klose, K.B., and Wilson, L., 1992, Steep-sided domes on Venus—Characteristics, geologic setting, and eruption conditions from Magellan data: Journal of Geophysical Research, v. 97, no. E8, p. 13445–13478, https://doi.org/10.1029/92JE01162.
Pettengill, G.H., Ford, P.G., Johnson, W.T.K., Raney, R.K., and Soderblom, L.A., 1991, Magellan—Radar performance and data products: Science, v. 252, no. 5003, p. 260–265, https://doi.org/10.1126/science.252.5003.260.
Pettengill, G.H., Ford, P.G., and Wilt, R.J., 1992, Venus surface radiothermal emissions observed by Magellan: Journal of Geophysical Research, v. 97, no. E8, p. 13091–13102, https://doi.org/10.1029/92JE01356.
Plaut, J.J., Anderson, S.W., Crown, D.A., Stofan, E.R., and van Zyl, J.J., 2004, The unique radar properties of silicic lava domes: Journal of Geophysical Research, v. 109, no. E3, article E03001, https://doi.org/10.1029/2002JE002017.
Roberts, K.M., Guest, J.E., Head, J.W., III, and Lancaster, M.G., 1992, Mylitta Fluctus, Venus—Rift-related, centralized volcanism and the emplacement of large-volume flow units: Journal of Geophysical Research, v. 97, no. E10, p. 15991–16016, https://doi.org/10.1029/92JE01245.
Saunders, R.S., Spear, A.J., Allin, P.C., Austin, R.S., Berman, A.L., Chandlee, R.C., Clark, J., Decharon, A.V., De Jong, E.M., Griffith, D.G., and 17 others, 1992, Magellan mission summary: Journal of Geophysical Research, v. 97, no. E8, p. 13067–13090, https://doi.org/10.1029/92JE01397.
Schaber, G.G., Strom, R.G., Moore, H.J., Soderblom, L.A., Kirk, R.L., Chadwick, D.J., Dawson, D.D., Gaddis, L.R., Boyce, J.M., and Russell, J., 1992, Geology and distribution of impact craters on Venus—What are they telling us?: Journal of Geophysical Research, v. 97, no. E8, p. 13257–13302, https://doi.org/10.1029/92JE01246.
Schultz, P.H., 1992, Atmospheric effects on ejecta emplacement and crater formation on Venus from Magellan: Journal of Geophysical Research, v. 97, no. E10, p. 16183–16248, https://doi.org/10.1029/92JE01508.
Senske, D.A., 1990, Geology of the Venus equatorial region from Pioneer Venus radar imaging: Earth, Moon, and Planets, v. 50, no. 1, p. 305–327, https://doi.org/10.1007/BF00142397.
Senske, D.A., Campbell, D.B., Stofan, E.R., Fisher, P.C., Head, J.W., III, Stacy, N., Aubele, J.C., Hine, A.A., and Harmon, J.K., 1991, Geology and tectonics of Beta Regio, Guinevere Planitia, Sedna Planitia, and Western Eistla Regio, Venus—Results from Arecibo image data: Earth, Moon, and Planets, v. 55, no. 2, p. 163–214, https://doi.org/10.1007/BF00058901.
Smrekar, S.E., Kiefer, W.S., and Stofan, E.R., 1997, Large volcanic rises on Venus, *in* Bougher, S.W., Hunten, D.M., and Phillips, R.J., eds., Venus II—Geology, geophysics, atmosphere, and solar wind environment: Tucson, Ariz., University of Arizona Press, p. 845–878.
Solomon, S.C., Smrekar, S.E., Bindschadler, D.L., Grimm, R.E., Kaula, W.M., McGill, G.E., Phillips, R.J., Saunders, R.S., Schubert, G., Squyres, S.W., and Stofan, E.R., 1992, Venus tectonics—An overview of Magellan observations: Journal of Geophysical Research, v. 97, no. E8, p. 13199–13256, https://doi.org/10.1029/92JE01418.
Squyres, S.W., Janes, D.M., Baer, G., Bindschadler, D.L., Schubert, G., Sharpton, V.L., and Stofan, E.R., 1992, The morphology and evolution of coronae on Venus: Journal of Geophysical Research, v. 97, no. E8, p. 13611–13634, https://doi.org/10.1029/92JE01213.
Stofan, E.R., Anderson, S.W., Crown, D.A., and Plaut, J.J., 2000, Emplacement and composition of steep-sided domes on Venus: Journal of Geophysical Research, v. 105, no. E11, p. 26757–26771, https://doi.org/10.1029/1999JE001206.
Stofan, E.R., and Brian, A.W., 2012, Geologic map of the Themis Regio quadrangle (V–53), Venus: U.S. Geological Survey Scientific Investigations Map 3165, 1 sheet, scale 1:5,000,000, 13-p pamphlet, https://doi.org/10.3133/sim3165.
Stofan, E.R., Hamilton, V.E., Janes, D.M., and Smrekar, S.E., 1997, Coronae on Venus—Morphology and origins, *in* Bougher, S.W., Hunten, D.M., and Phillips, R.J., eds., Venus II—Geology, geophysics, atmosphere, and solar wind environment: Tucson, Ariz., University of Arizona Press, p. 931–965.
Stofan, E.R., Head, J.W., III, and Campbell, D.B., 1990, Beta-Eistla deformation zone: analysis from recent Arecibo images [abs.], *in* 21st Lunar and Planetary Science Conference, Houston, Tex., March 12–16, 1990, Abstracts: Lunar and Planetary Science Conference, abstract 1613, p. 1208-1209.
Stofan, E.R., Head, J.W., III, Campbell, D.B., Zisk, S.A., Bogomolov, A.F., Rzhiga, O.N., Basilevsky, A.T., and Armand, N., 1989, Geology of a rift zone on Venus—Beta Regio and Devana Chasma: Geological Society of America Bulletin, v. 101, no. 1, p. 143–156, https://doi.org/10.1130/0016-7606(1989)101<0143:GOARZO>2.3.CO;2.
Stofan, E.R., Sharpton, V.L., Schubert, G., Baer, G., Bindschadler, D.L., Janes, D.M., and Squyres, S.W., 1992, Global distribution and characteristics of coronae and related features on Venus—Implications for origin and relation to mantle processes: Journal of Geophysical Research, v. 97, no. E8, p. 13347–13378, https://doi.org/10.1029/92JE01314.
Tanaka, K.L., Senske, D.A., Price, M., and Kirk, R.L., 1997, Physiography, geomorphic/geologic mapping and stratigraphy of Venus, *in* Bougher, S.W., Hunten, D.M., and Phillips, R.J., eds., Venus II—Geology, geophysics, atmosphere, and solar wind environment: Tucson, Ariz., University of Arizona Press, p. 667–694.
Wilhelms, D.E., 1972, Geologic mapping of the second planet: U.S. Geological Survey Interagency Report—Astrogeology 55.
Wilhelms, D.E., 1990, Geologic mapping, *in* Greeley, R., and Batson, R.M., eds., Planetary mapping: New York, N.Y., Cambridge University Press, p. 208–260.